Supplementary Material (ESI) for Soft Matter

Molecular Dynamics Simulations of the Interactions of Charge-neutral PAMAM Dendrimers with the Pulmonary Surfactant

Xubo Lin[1, 2], Yang Li[3] and Ning Gu[1, 2, *]

1. School of Biological Science & Medical Engineering, Southeast University, Nanjing, 210096, P. R. China
2. State Key Laboratory of Bioelectronics and Jiangsu Laboratory for Biomaterials and Devices, Nanjing, 210096, P. R. China
3. Department of Biomedical Engineering, Tianjin Medical University, Tianjin, 300070, P. R. China

* Corresponding author. E-mail: guning@seu.edu.cn.

Ⅰ. SUPPLEMENTARY METHODS

Force Field

According to the force field[1, 2], four different CG sites are considered: charged (Q), polar (P), nonpolar (N), and apolar (C). Subscripts are used to further distinguish groups with different chemical nature: 0, no hydrogen-bonding capabilities are present; d, groups acting as hydrogen bond donor; a, groups acting as hydrogen bond acceptor; da, groups with both donor and acceptor options; 1-5, indicating increasing polar affinity. DPPC consists of four bead types: Q0, Qa, Na and C1. Water: P4; Charge-neutral PAMAM dendrimer[3, 4]: N0 and Nda. Dendrimers consist of a core molecule and alternating layers of two monomers (here refers to N_0 and Nda). Each pair of monomer layers completes a shell and a generation. Fig. S1 shows the structure of G3 PAMAM dendrimer. G5 and G7 PAMAM dendrimers can be described by repeating monomer layers. Fig. S2 show the coarse-grained structures of DPPC molecule and water molecules. Table S1 describes the interaction parameters between PAMAM dendrimer and DPPC, water. We can find PAMAM dendrimer have generally attractive interactions with DPPC and water except for the hydrophobic tail of DPPC. For acetylated dendrimers focused on in our simulations, there are little differences in long-range and short-range treatments of electrostatics[3, 4]. We also try long-range particle mesh Ewald (PME) electrostatics for system G7-1, which shows little differences with the same system using a short-range electrostatic cutoff (data not shown). Besides, in previous bi-monolayer system (used for pulmonary surfactant) modeling[8], a short-range electrostatic cutoff is widely used. Thus, we choose a short-range electrostatic cutoff for our simulations.

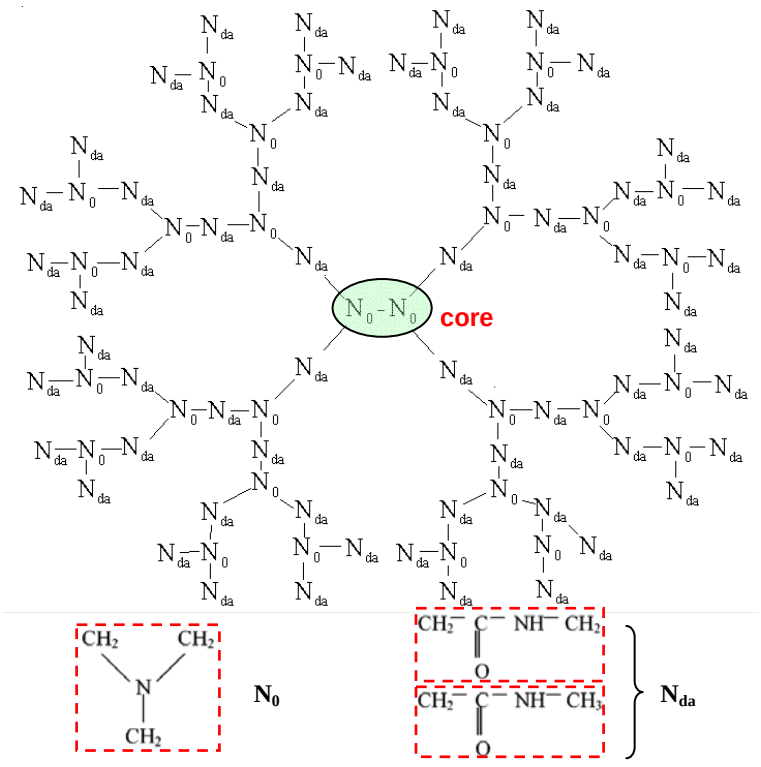

Fig. S1 Schematic of coarse-grained (CG) charge-neutral G3 PAMAM dendrimer's structure

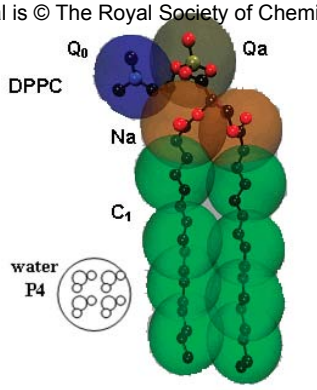

Fig. S2 Schematic of coarse-grained DPPC and water's structures[1]

TABLE S1: Interaction Matrix [a]

		DPPC				water
		Q_0	Qa	Na	C_1	P_4
PAMAM dendrimer	Nda	III	I	II	VI	III
	N_0	IV	IV	IV	VI	IV

[a] Level of interaction indicates the well depth in the LJ potential: O, ε=5.6 kJ/mol; I, ε=5.0 kJ/mol; II, ε=4.5 kJ/mol; III, ε=4.0 kJ/mol; IV, ε=3.5 kJ/mol; V, ε=3.1 kJ/mol; VI, ε=2.7 kJ/mol; VII, ε=2.3 kJ/mol; VIII, ε=2.0 kJ/mol; IX, ε=2.0 kJ/mol. The LJ parameter σ=0.47 nm for all interaction levels except level IX for which σ=0.62 nm.

I: attractive; II: almost attractive; III: semi attractive; IV: intermediate; VI: semi repulsive

Order parameter

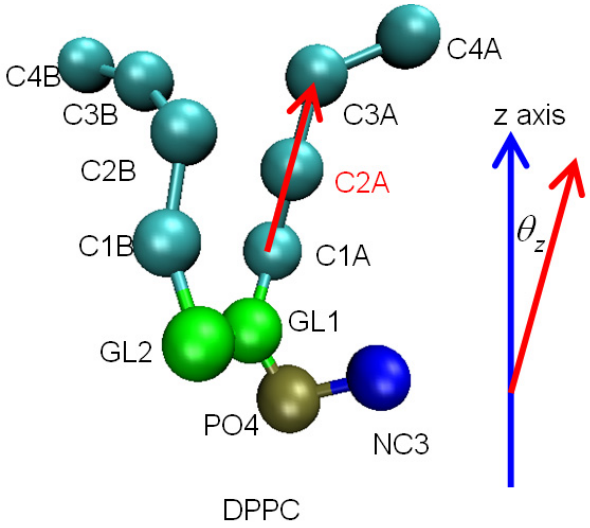

Fig. S3 Schematic of our vector defined for DPPC CG model. Take the bead C2A as the reference point, then the vector is shown in red arrow.

To understand the phase behavior of the interface DPPC monolayer under the effect of different PAMAM dendrimers, we further calculate the order parameter using the equation $S_z = \frac{3}{2}\left\langle \cos^2 \theta_z \right\rangle - \frac{1}{2}$, where θ_z is the angle between the interface normal (in our simulation, it's the z-axis of the simulation box) and the vector connecting adjacent two beads C_{n-1}, C_{n+1} (We do not use the vector definition in reference[5] for CG model but adopt this definition similar to that described in GROMACS manual[6]. An example is shown in Fig. S3.). The bracket implies averaging over all interface DPPC molecules and time. Order parameters can vary between 1 (uniformly orientated in the interface normal direction) and -1/2 (uniformly orientated perpendicular to the normal).

Averaged Radial Area per Lipid:

To calculate the radial average area per lipid (Aav), we use the c.o.m. of the PAMAM dendrimer as the center and construct a series of concentric rings. Then we count the number of the DPPC heads (We choose PO4 bead type) in each concentric ring. By dividing the area of each concentric ring with corresponding number, we obtain radial area per lipid average over molecules. The corresponding radius (r) value is set as the middle of the ring. Further, we average this area per lipid over a selected time period to obtain the value averaged over molecules and time. By the way, the periodic boundary conditions are considered in this calculation. For example, the green part of Fig. S4 is a concentric ring, with O as the center, A as the middle point of ring width. Suppose that the area of this ring is S_t and the number of the PO4 beads in it is N_t, then we can obtain the radial area per lipid at r=OA: $Aav =< S_t / N_t >$, where the bracket represents average over time.

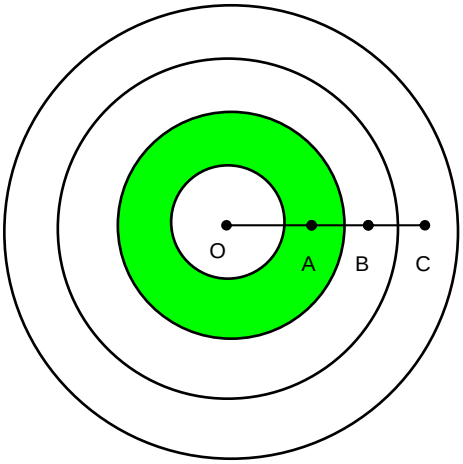

Fig. S4 Schematic diagram for calculating radial area per lipid. AB=2Δr

We choose Δr=0.5nm for the calculation of Aav based on the relationship between Aav, its error bar and Δr (Fig. S5). Aav and its error bar converge at Δr=0.5nm fairly well.

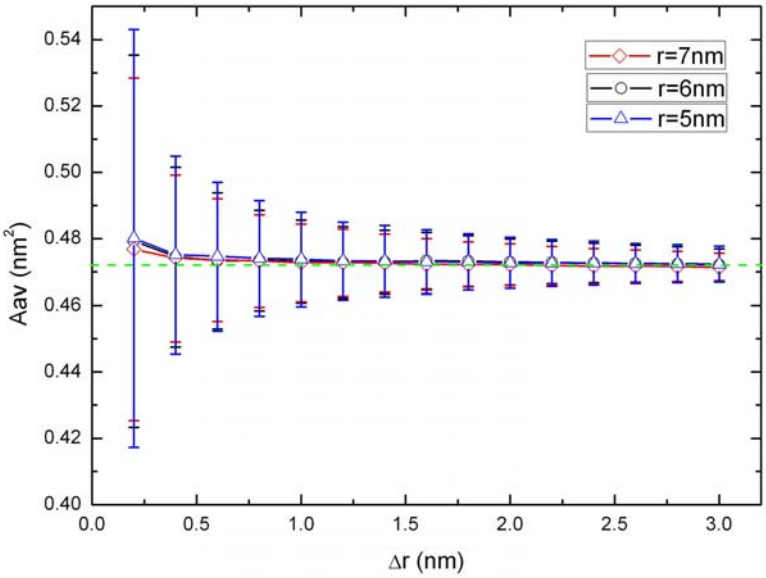

Fig. S5 The radial average area per lipid (Aav), its error bar v.s. Δr at three different radial positions.

Ⅱ. SUPPLEMENTARY FIGURES AND DISCCUSION

The definition of the interfacial molecules

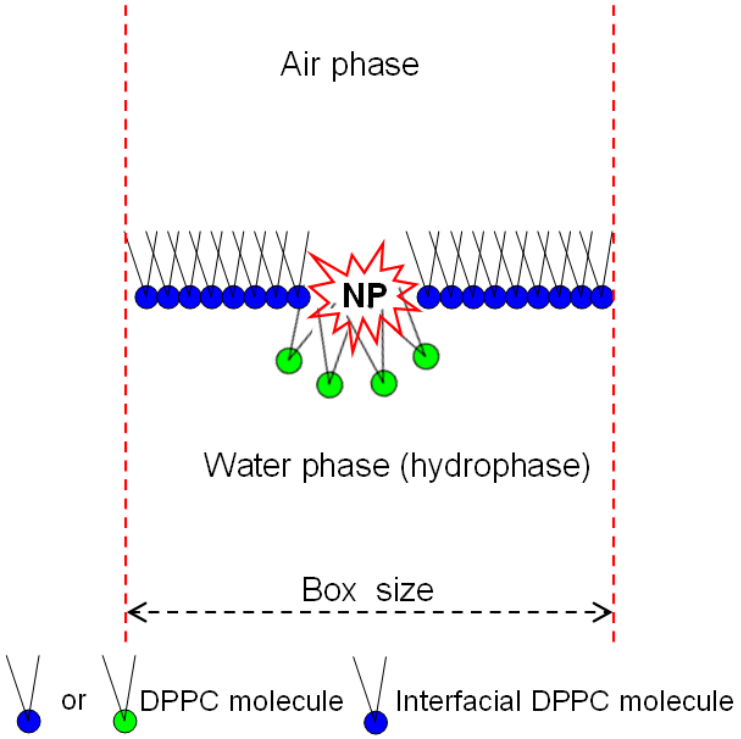

Fig. S6 Schematic of the interfacial molecules.

Time evolution of the box sizes of all simulation systems

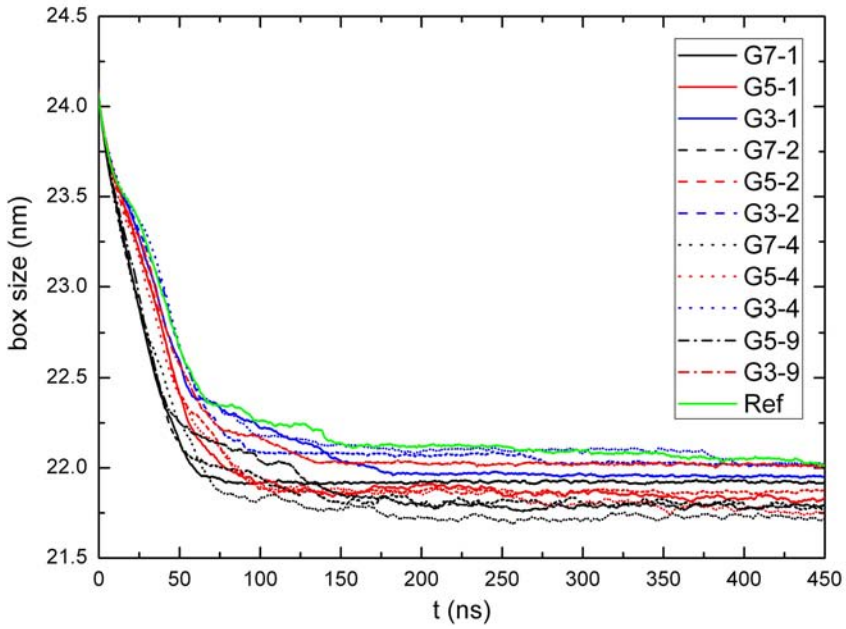

Fig. S7 Time evolution of the box sizes of all simulation systems during compression.

Structural disruption of single PAMAM dendrimer on the DPPC monolayer

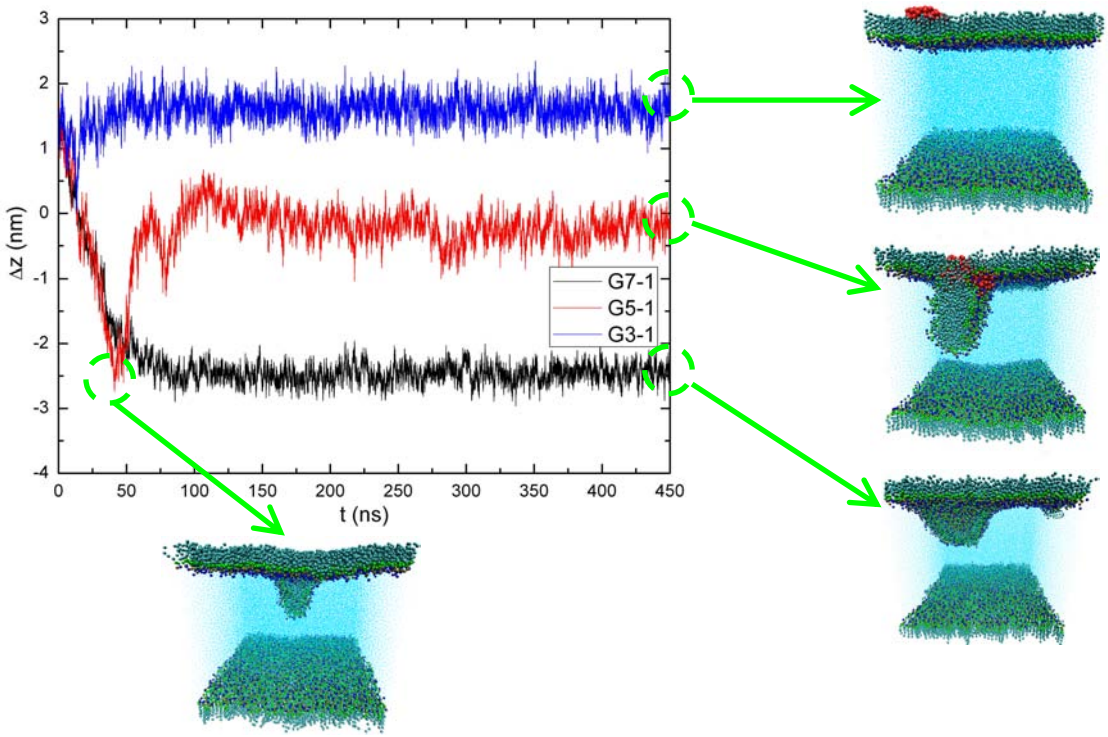

Fig. S8 Time evolution of the distance (Δz) between c.o.m. of PAMAM dendrimer and c.o.m. of interface DPPC molecules along z-axis. The black line is for system G7-1, the red for G5-1, the blue for G3-1.

Fig. S8 is more figurative than Fig. 2 in our manuscript. The differences of these three systems' conformation transformations are as follows: 1) G7-1: a→b; 2) G5-1: a→b→c; 3) G3-1: a→b→a (States a, b, c are described in Fig. 1. a: PAMAM dendrimer adsorbs onto the DPPC monolayer; b: buckling structure[8, 9]; c: "fold" structure[8, 9]). In order to evaluate the possibility of further transformation of G7-1, we extend the simulation length of G7-1 to 800ns (Fig. S9). The result shows that the buckling structure of system G7-1 is rather stable, which is consistent with the trend of the time-evolution of box size, Δz and vdW interaction energy.

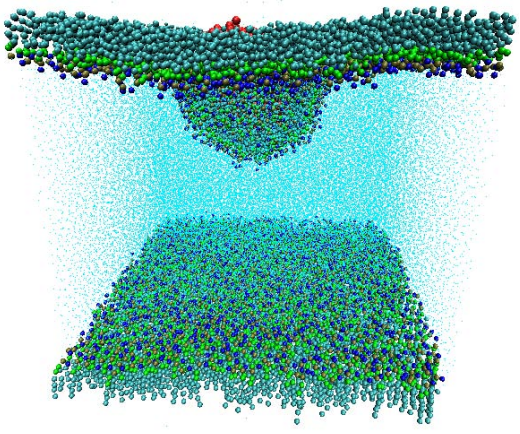

Fig. S9 Snapshot of the system G7-1 at 800ns.

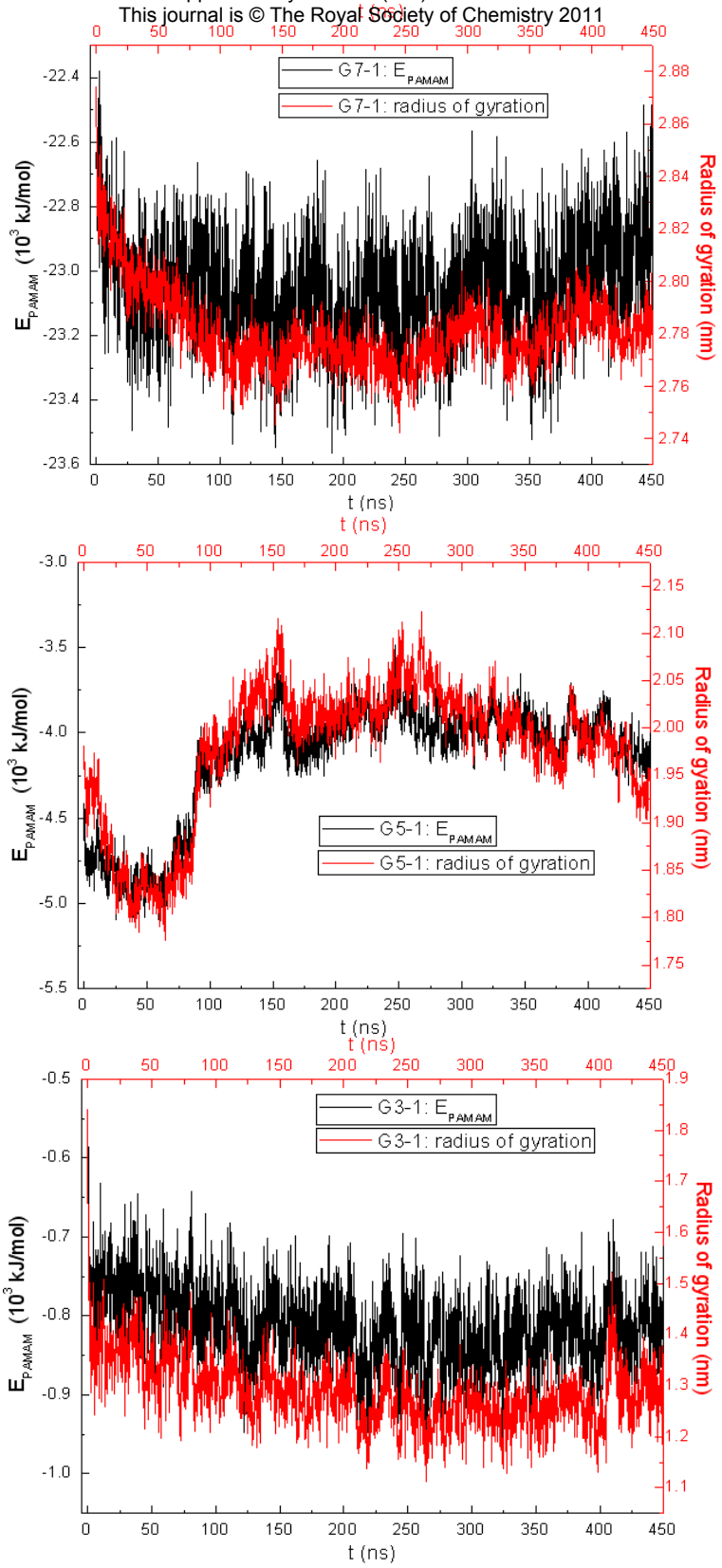

Fig. S10 Time evolution of E_{PAMAM} and radius of gyration for systems G7-1, G5-1 and G3-1.

Details of the system G7-4

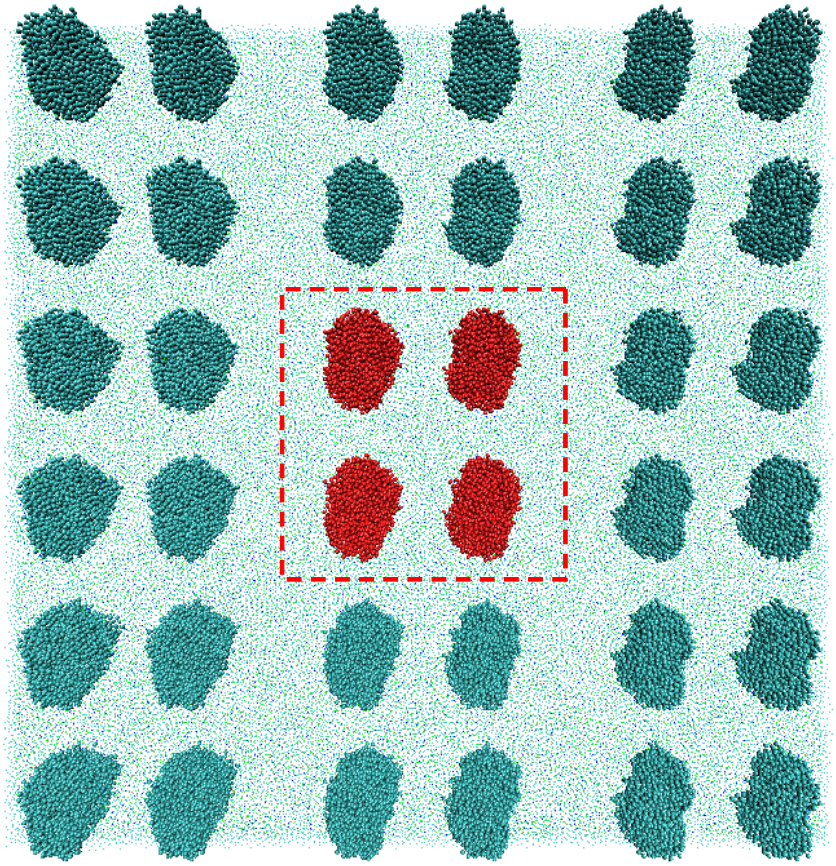

Fig. S11 Snapshot of G7-4 at the initial time with its 8 period mirror images on.

From Fig. 8 in our manuscript, it seems as if G7 PAMAM dendrimers had contacted each other considering pbc conditions. Thus we show the snapshot of this system together with its period mirror images in Fig. S11 to confirm G7 PAMAM dendrimers do not contact each other at all at initial time. It is just a problem of the visualization of the software VMD.

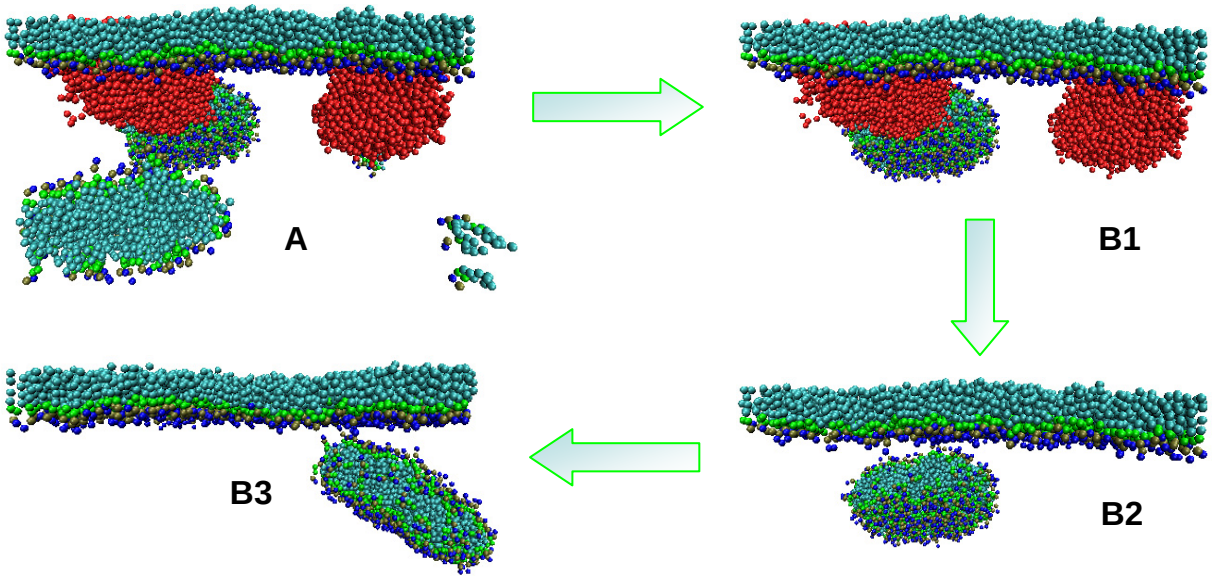

Fig. S12 Details of the detached fold structure appeared in system G7-4. (A) Direct visualization of the last frame of G7-4; (B1) Translating the fold structure considering the pbc condition; (B2) and (B3) is the visualization of (B1) after removing G7 PAMAM dendrimers at different angles. Water molecules are not shown for clarity.

Normal phase transition of the DPPC monolayer at the air-water interface during the compression process[7]

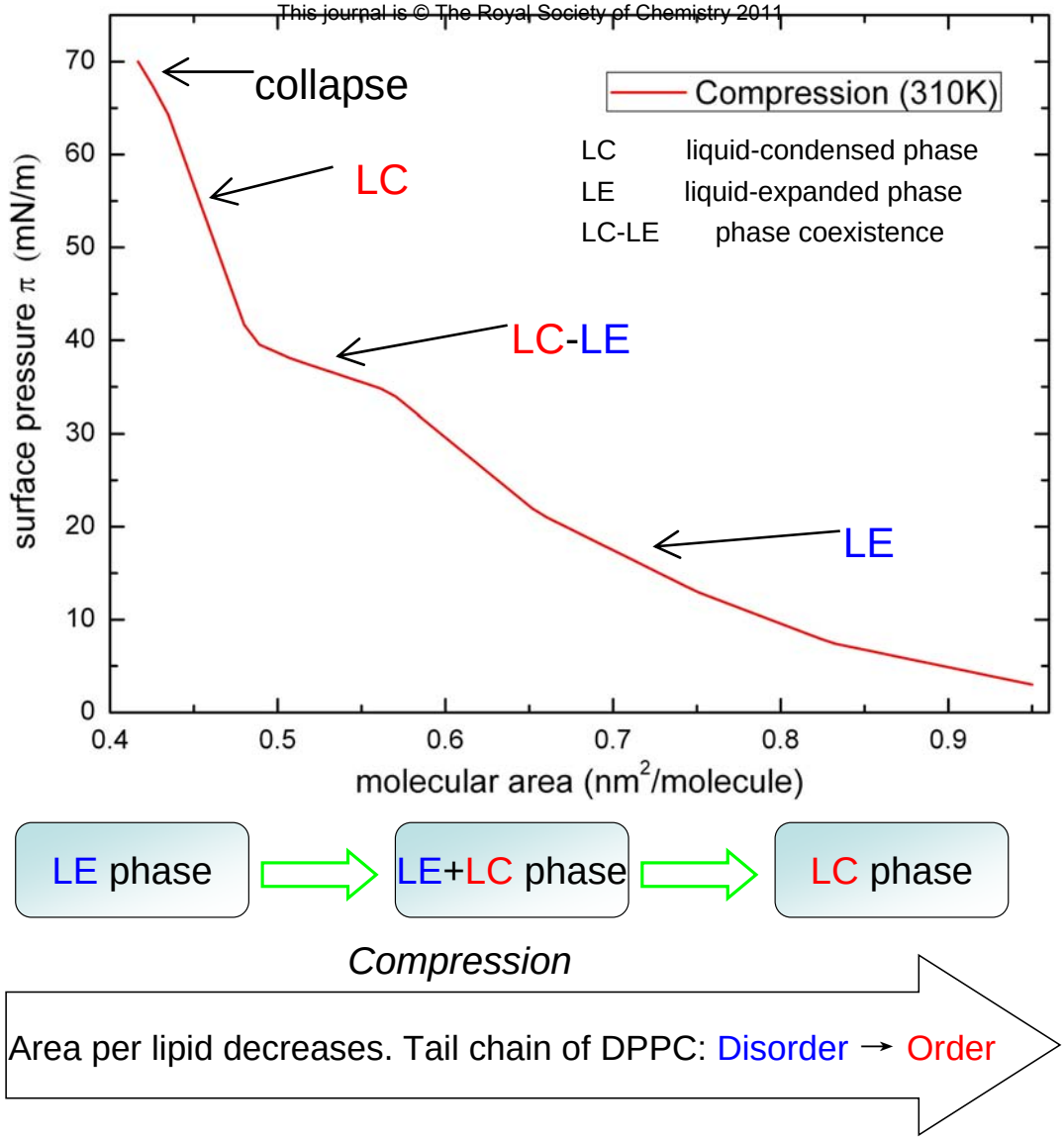

Fig. S13 Phase transition of the pure interfacial DPPC molecules at air-water interface during compression.

References:

[1] S. J. Marrink, A. H. de Vries, A. E. Mark, *J. Phys. Chem. B*, 2004, 108, 750-760
[2] S. J. Marrink, H. J. Risselada, S. Yefimov, D. P. Tieleman, A. H. de Vries, *J. Phys. Chem. B*, 2007, 111, 7812-7824
[3] H. Lee, R. G. Larson, *J. Phys. Chem. B*, 2006, 110, 18204-18211
[4] H. Lee, R. G. Larson, *J. Phys. Chem. B*, 2008, 112, 7778-7784
[5] C. Laing, S. Baoukina, D. P. Tieleman, *Phys. Chem. Chem. Phys.*, 2009, 11, 1916-1922
[6] D. van der Spoel, E. Lindahl, B. Hess, A. R. van Buuren, E. Apol, P. J. Meulenhoff, D. P. Tieleman, A. L. T. M. Sijbers, K. A. Feenstra, R. van Drunen, H. J. C. Berendsen, Gromacs User Manual version 4.0, www.gromacs.org (2005)
[7] J. M. Crane, G. Putz, S. B. Hall, *Biophysical Journal*, 1999, 77, 3134-3143
[8] S. Baoukina, L. Monticelli, H. J. Risselada, S. J. Marrink, D. P. Tieleman, *Proc. Natl. Acad. Sci. USA*, 2008, 105, 10803-10808
[9] B. Piknova, V. Schram, S. B. Hall, *Current Opinion in Structural Biology*, 2002, 12, 487-494